

Research Article

Mechanism of Yangxin Tongmai Decoction in the Treatment of Coronary Heart Disease with Blood Stasis Syndrome Based on Network Pharmacology and Molecular Docking

Mengxue Zhang ^{1,2}, Jia Liu ¹, Xiangzhuo Zhang ¹, Shumeng Zhang ¹, Yujie Jiang ¹,
Zixuan Yu ¹, Ting Xie ¹, Yuxia Chen ¹, Lingli Chen ³ and Jie Li ¹

¹Hunan University of Traditional Chinese Medicine, Hunan Changsha 410208, China

²Longhua Hospital, Shanghai University of Traditional Chinese Medicine, Shanghai 200032, China

³Hunan Provincial Key Laboratory of Pathogenic Biology Based on Integrated Chinese and Western Medicine, Hunan University of Chinese Medicine, Hunan Changsha 410208, China

Correspondence should be addressed to Lingli Chen; linglichen02@sina.com and Jie Li; 317768870@qq.com

Received 10 May 2022; Revised 30 July 2022; Accepted 10 August 2022; Published 30 September 2022

Academic Editor: Talha Bin Emran

Copyright © 2022 Mengxue Zhang et al. This is an open access article distributed under the Creative Commons Attribution License, which permits unrestricted use, distribution, and reproduction in any medium, provided the original work is properly cited.

This study aimed to explore the mechanism of Yangxin Tongmai decoction (YXTMD) in the treatment of coronary heart disease (CHD) with blood stasis syndrome (BSS) using network pharmacology and molecular docking, and to verify these results through clinical trials. The active compounds of YXTMD were identified using the Traditional Chinese Medicine Systems Pharmacology database, and the targets of the active compounds were predicted using the SwissTarget Prediction database. The targets of CHD and BSS were predicted using the GeneCards, OMIM, PharmGKB, TTD, and DrugBank databases. The common targets of “herb-disease-phenotype” were obtained using a Venn diagram, then used Cytoscape software 3.8.2 and its plug-in CytoNCA and STRING database to construct the “herb active compounds-common target” and protein–protein interaction networks. R language software and bioconductor plug-in were used for Gene Ontology (GO) and Kyoto Encyclopedia of Genes and Genomes (KEGG) enrichment analyses. AutoDock was used for the molecular docking analysis. Finally, clinical trials were conducted to confirm the results of network pharmacology. Eighty-three active components were obtained, and the core active components were 5,7,4'-trimethoxyflavone, tetramethoxyluteolin, isosinensetin, sinensetin, and 5,7-dihydroxy-2-(3-hydroxy-4-methoxyphenyl)chroman-4-one. A total of 140 common targets were identified, and the core targets were EGFR, VEGFA, AKT1, STAT3, TP53, ERBB2, and PIK3CA. Biological processes identified by the GO analysis primarily involved wound healing, regulation of body fluid levels, and vascular process in circulatory system. The cellular components were primarily located in the membrane raft, membrane microdomain, and plasma membrane raft. The primary molecular functions were activity of transmembrane receptor protein kinase, transmembrane receptor protein tyrosine kinase, and protein tyrosine kinase. KEGG analysis showed that the PI3K-Akt signaling pathway was closely related to the treatment of CHD with BSS by YXTMD. Molecular docking results showed that the core active components had a good binding activity with the core targets. The clinical trial results showed that YXTMD improved the BSS scores and decreased the serum levels of total cholesterol and low-density lipoprotein cholesterol. Moreover, the levels of *PI3k* and *AKt* mRNA were upregulated and the levels of *GSK-3β* mRNA were downregulated. YXTMD has multicomponent, multitarget, and multipathway effects in the treatment of CHD with BSS, and its mechanism of action may involve activation of the PI3K-Akt signaling pathway, downregulation of *GSK-3β*, and mediation of in vivo lipid metabolism-based metabolic processes.

1. Introduction

Coronary heart disease (CHD) is caused by coronary artery atherosclerosis or spasms. This condition triggers stenosis or occlusion of the lumen, resulting in myocardial ischemia and hypoxia as well as clinical symptoms such as chest pain and tightness [1]. The World Health Organization (WHO) estimated that the number of people who died of cardiovascular disease worldwide accounted for approximately one-third of all deaths in 2019, among which ischemic heart disease was the most common [2]. The morbidity and mortality rates of CHD are likely to continue to grow due to the aging of the population, thereby seriously threatening human health and becoming a global public health burden [3]. The main clinical treatment for this disease is drug therapy, including lipid-regulating and stabilizing drugs, antiplatelet aggregation and thrombosis drugs, anticoagulant drugs, nitrate drugs, and β -receptor blockers [4]. Although these drugs can improve symptoms and delay disease progression, they have a single target of action and drug combinations are often required. Some patients also experience side effects after long-term use, such as liver and kidney function damage, bleeding, and hypotension [5, 6]. Therefore, other therapeutic drugs still need to be actively explored.

A wide range of Chinese herbal medicines exist with fewer toxic side effects than western medicine [7, 8]. They have the characteristics of being multicomponent, multi-target, and multipathway in the treatment of diseases, which can compensate for the limitations of a single Western medical treatment. In particular, Chinese herbal medicines have unique advantages in preventing and treating CHD [9, 10]. At the same time, it can reduce the side effects of Western medicine [11]. CHD belongs to the traditional Chinese medicine (TCM) category of “chest obstruction, cardiac pain, and genuine heart pain,” and its key pathogenesis is “the obstruction of cardiac vessels (Xin Mai Bu Tong).” The principle of TCM is “discriminatory treatment.” With the increasing number of studies on TCM syndromes, more researchers are exploring new ways to treat diseases from this perspective. Blood stasis syndrome (BSS) is the most common type of CHD [12] and is a research hotspot in the current mode of disease-syndrome combination. Yangxin Tongmai decoction (YXTMD) was developed by a renowned TCM physician, Mr. Bowei Qin, and is an effective prescription for treating cardiovascular diseases [13]. Subsequently, Professor Zhaokai Yuan modified it according to the theory of “nourishing heart Qi (Fu Yang Xin Qi) and re-establishing blood circulation (He Tong Xue Mai).” YXTMD comprises five drugs: renshen (*Radix Ginseng*), guizhi (*Ramulus Cinnamomi*), danshen (*Radix Salviae Miltiorrhizae*), zhishi (*Fructus Aurantii Immaturus*), and zexie (*Rhizoma Alismatis*). Preliminary clinical and experimental studies have confirmed that YXTMD prescription can relieve angina pectoris and antimyocardial ischemia, lower blood lipids, inhibit inflammatory response, activate platelet aggregation, promote coronary angiogenesis, and increase coronary blood flow [14–16]. Although the therapeutic effect of YXTMD is exact, its main active ingredients

and mechanisms of action in the treatment of CHD with BSS have not been fully clarified due to its multitarget action.

Network pharmacology is used to study drugs and their targets and pharmacological activities based on a “drug component–target–disease” interaction network. This network can clarify the mechanism of action of drugs in the treatment of diseases from a holistic perspective and provide new ideas for research on Chinese herbal medicines and their compounds. We therefore aimed to explore the active ingredients, key targets, and specific mechanisms of action of YXTMD in the treatment of CHD with BSS using network pharmacology and molecular docking technology. These results were further verified in clinical trials to provide a theoretical basis for the development and clinical application of the drug. The detailed workflow of the study is shown in Figure 1.

2. Materials and Methods

2.1. Active Compounds and Targets of YXTMD. The Traditional Chinese Medicine Systems Pharmacology (TCMSP) database [17] (<https://tcmssp.com/tcmssp.php>) was used to identify the chemical components of YXTMD, including renshen, guizhi, danshen, zhishi, and zexie. Oral-bioavailability (OB) [18] $\geq 30\%$ and drug-likeness (DL) [19] ≥ 0.18 were used as parameters to determine the active compounds of YXTMD. The PubChem [20] (<https://pubchem.ncbi.nlm.nih.gov/>) database was used to collect and collate candidate compounds, and the data were saved in SDF format as 2D or 3D structures. Swisstarget prediction [21] (<https://www.swisstargetprediction.ch/>) was used to predict the target of the active compounds by setting the species as “Homo sapiens.” Meanwhile, compounds without chemical structures and targets were eliminated, and the UniProt (<https://www.uniprot.org/>) database was used to standardize potential targets.

2.2. Targets of CHD with BSS and Common Targets of “YXTMD-CHD-BBS”. The GeneCards (<https://www.genecards.org/>), OMIM (<https://omim.org/>), PharmGkb (<https://www.pharmgkb.org/>), Therapeutic Target (TTD) (<https://db.idrblab.net/ttd/>), and DrugBank (<https://www.drugbank.ca/>) databases were used to collect the targets of the disease and phenotype. We set “coronary heart disease” and “blood stasis syndrome” as the keywords. Related target genes were merged and duplicate values removed to obtain the related targets of CHD with BSS. The common targets of “YXTMD-CHD-BBS” were obtained using VandePeer Labin Bioinformatics Gent (<https://bioinformatics.psb.ugent.be/beg/>), and a Venn diagram was drawn.

2.3. Network Construction of “Active Components of YXTMD-Common Targets”. Cytoscape 3.8.2 software was used to construct a network model of “active components of YXTMD-common targets.” The network diagram was analyzed using a network analyzer to obtain the degree ranking of active components.

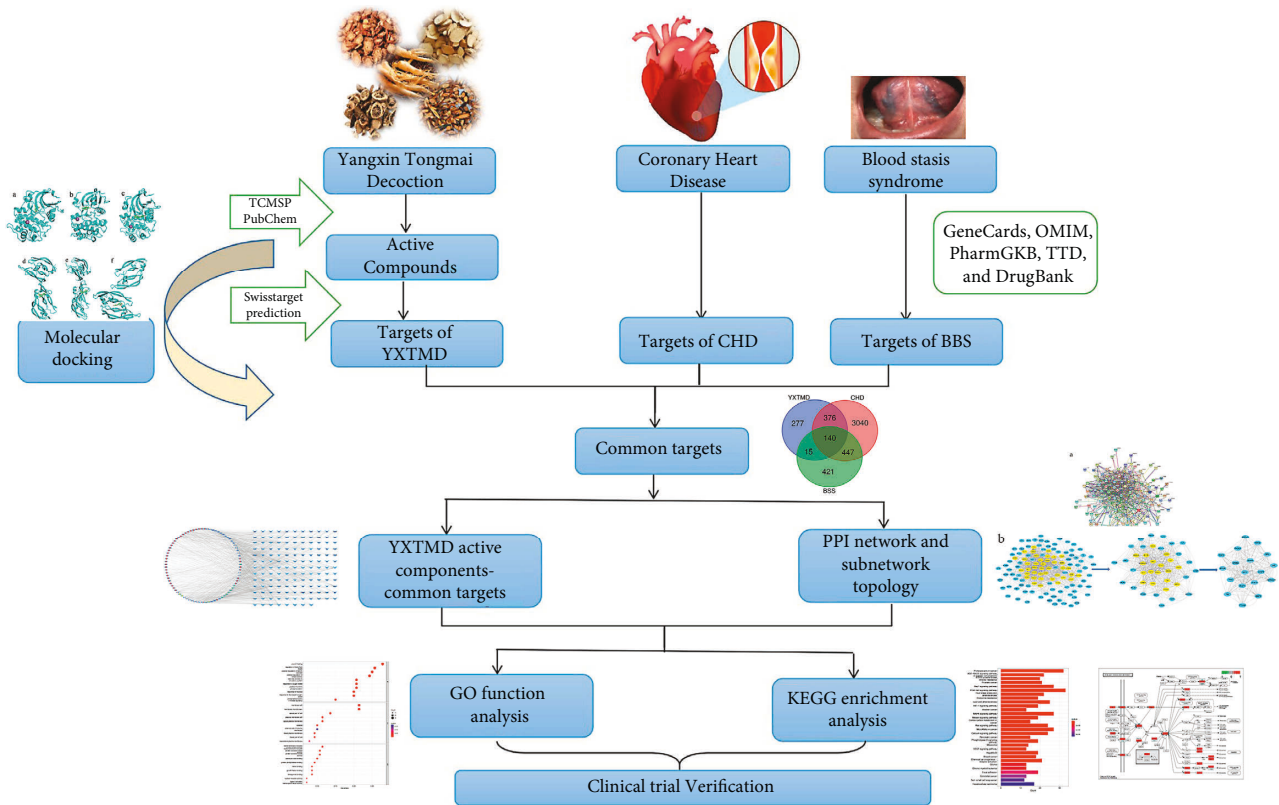


FIGURE 1: The workflow used in the study.

2.4. Protein-Protein Interaction Network. Common targets were imported into the STRING [22] (<https://string-db.org/>) database, and the research species was set as “*Homo sapiens*.” The minimum confidence score was 0.700 [23] and a network diagram of protein-protein interactions (PPI) was obtained. The protein interaction data were imported into Cytoscape 3.8.2, and the algorithms of betweenness, closeness, degree, eigenvector, and the local average connectivity-based method and network in CytoNCA were used for topological analysis [24]. The core gene was screened

2.5. Gene Ontology and Kyoto Encyclopedia of Genes and Genomes Pathway Enrichment Analysis. Gene ontology (GO) and Kyoto Encyclopedia of Genes and Genomes (KEGG) pathway enrichment analyses were performed using R software and the bioconductor plug-in with a screen condition of $P < 0.05$. The top ten items were selected for visualization, and a bar diagram and bubble diagram were drawn.

2.6. Molecular Docking. The 2D structures of the active components were downloaded from the PubChem database and saved in mol2 format using ChemBio3D Ultra software. The pdb formats of the 3D structures of the targets were downloaded from the Protein Data Bank (PDB) (<https://www.rcsb.org/>) based on the core gene target IDs found in the UniProt database. The PyMOL software was used to remove water molecules, and hydrogen atoms were added to the targets. AutoDock software was used to convert the format of active components and target proteins into the

pdqbt format. Finally, molecular docking was performed using AutoDock Vina software and the results were visualized using PyMOL software. A binding energy less than “5 kcal/mol” was used to indicate a good binding interaction between the compound and the target [25].

2.7. Verification of Clinical Trial

2.7.1. Participants. A total of 26 patients with CHD with BSS admitted to the cardiovascular department of the First Affiliated Hospital of Hunan University of Chinese Medicine between April 2021 and January 2022 were recruited for this study. This study was approved by the Ethics Committee of the First Affiliated Hospital of Hunan University of Chinese Medicine (No. HN-LL-GZR-201820).

(1) Diagnostic criteria

CHD was diagnosed according to the “Guidelines for the Diagnosis and Treatment of Chronic Stable Angina Pectoris” [26] and “Guidelines for the Diagnosis and Treatment of Unstable Angina Pectoris and Non-ST-elevation Myocardial Infarction” [27] established by the Chinese Medical Association Cardiovascular Branch in 2007. Coronary angiography revealed at least one coronary artery with $\geq 50\%$ luminal diameter. BSS was diagnosed according to the “Diagnostic Criteria of Coronary Heart Disease with BSS” formulated by the committee of promoting blood circulation and removing blood stasis in 2016 [28].

(2) Inclusion criteria

Patients who met the above diagnostic criteria for CHD and BSS, had complete clinical data, and voluntarily participated in the study and provided informed consent were included in the study.

(3) Exclusion criteria

Excluded from the study were patients with severe heart disease (thyroid-related cardiomyopathy, hypertensive heart disease, anemic heart disease, pulmonary heart disease, rheumatic heart disease, etc.); those with malignant tumors, blood system diseases, connective tissue diseases, mental disorders, tuberculosis, and other infectious diseases; those with serious complications of liver and kidney dysfunction; those with poor compliance and incomplete clinical test data; and those who refused to accept the study and provide informed consent.

2.7.2. Main Instruments and Reagents. The following instruments and reagents were used: a fluorescence quantitative PCR instrument; fluorescence PCR plate (Thermo Fisher Scientific, Waltham, MA, USA); desktop freezing centrifuge (Xiangyi, Hunan, China); electrophoresis instrument; horizontal agarose electrophoresis tank (Liuyi, Beijing, China); biological sample homogenizer (Aosheng, Hangzhou, China); enzyme-labeling analyzer (Jiancheng Bioengineering Research Institute, Nanjing, China); ultra-microspectrophotometer (Baoyude Scientific Instrument, Shanghai, China); mRNA reverse-transcription kit (Code No. CW2569; Kangwei Century, Beijing, China); superoxide dismutase (SOD), nitric oxide (NO), and malondialdehyde (MDA) enzyme-linked immunosorbent assay (ELISA) kits (Code No. A001-3, A013-2, and A003-1; Jiancheng Bioengineering Research Institute, Nanjing); tumor necrosis factor- α (TNF)- α and interleukin-1 β (IL)-1 β ELISA kits (Code No. ml077385-2 and ml058059-2; enzyme-linked organisms, Shanghai, China); ethylenediaminetetraacetic acid (EDTA) (Code No. MB2514; Meilun, Dalian, China); Tris (Code No. V900483; Sigma-Aldrich, St. Louis, MO, USA); Trizol (Code No. 15596026; Thermo Fisher Scientific); UltraSYBR (Code No. CW2601; Kangwei Century, Beijing, China); and a blood collection needle and 5 ml blood collection tube (Sanli Medical Technology, China).

2.7.3. Research Methods

(1) Trial group

Data from 14 eligible patients were collected according to the criteria for diagnosis, inclusion, and exclusion. Patients were divided into two groups according to the random-number table method: the control group ($n=7$) and the treatment group ($n=7$). The control group included 5 males and 2 females (average age = 64.14 ± 4.95 years), and the treatment group included 5 males and 2 females (average age = 59.29 ± 5.94 years). No significant differences were observed in the general data between the two groups ($P > 0.05$).

(2) Treatment

Patients in the control group were administered routine western medicine, including aspirin enteric-coated tablets (100 mg by mouth per day [po qd]), atorvastatin calcium tablets (20 mg po qd), metoprolol succinate sustained-release tablets (23.75 mg po qd), and benazepril hydrochloride tablets (5 mg po qd). Antiangina drugs were discontinued during the treatment period. If angina pectoris broke out, nitroglycerin tablets were administered sublingually as appropriate.

Patients in the treatment group were administered YXTMD combined with routine western medicine. The YXTMD comprised Radix Panacis Quinquefolii (6 g), Ramulus Cinnamomi (8 g), Radix Salviae Miltiorrhizae (10 g), Fructus Aurantii Immaturus (10 g), and Rhizoma Alismatis (10 g). All Sanjiu granule types were produced by China Resources Sanjiu Pharmaceutical Co. Ltd. and one dose was administered per day and taken twice.

The treatment period for the two groups was 28 days. Patients were evaluated before and after treatment to determine the curative effects of the drugs according to the "Evaluation Criteria of Angina Pectoris and Electrocardiogram in Coronary Heart Disease" [29] and "Efficacy Evaluation Criteria for Coronary Heart Disease Angina Pectoris with Blood Stasis Syndrome" [30].

(3) Sample collection

Before and after treatment, 12 mL of elbow venous blood was taken from each patient after 8 h of fasting using a red common tube, sodium citrate blood collection tube, and EDTA-K2 anticoagulant blood collection tube. An ice-bag incubator was used to transport the blood samples, of which 4 ml was sent to the biochemical laboratory of the First Affiliated Hospital of Hunan University of Chinese Medicine within 2 h to determine the level of blood lipids. The remaining 8 mL was sent to the Intermediate Diagnosis Laboratory of Hunan University of Chinese Medicine within 2 h; 4 mL was poured into a cryopreservation tube, and the remaining 4 mL was centrifuged. The serum was poured into a cryopreservation tube, and all samples were stored at -80°C .

2.7.4. Index Determination

(1) ELISA

Blood samples were strictly analyzed according to the manufacturer's instructions. The curve formula was calculated using the standard concentration and absorbance (OD value) of the standard well. The measured OD values were substituted into the corresponding curve formulas to calculate the concentration of MDA, SOD, NO, TNF- α , and IL-1 β .

(2) Real-time PCR

Total RNA was extracted from the whole blood and reverse transcribed into cDNA. Finally, fluorescence quantitative PCR was performed to determine the expression levels of *PI3k*, *AKt*, *NF-κB*, *eNOS*, and *GSK-3β* mRNA. The steps of the reaction included an initial denaturation at 95°C for 10 min, followed by 40 cycles of denaturation at 95°C for 15 s and annealing at 60°C for 30 s. GAPDH served as an internal control, and gene expression was analyzed by the $2^{-\Delta\Delta C_t}$ method. Primer sequences were designed using Primer 5 and synthesized by Shanghai Bioengineering (Table 1).

2.7.5. Statistical Analysis. SPSS26.0 software was used for statistical analysis. Data are expressed as the mean \pm standard deviation ($\bar{x} \pm s$). For normally distributed data, the *t*-test was used when the variance was homogeneous and the Wilcoxon test was used when the variance was not homogeneous. Count data are expressed as frequency (constituent ratio,%), and comparisons between two groups were analyzed using the χ^2 test or Fisher's exact test was appropriate. Statistical significance was set at $P < 0.05$.

3. Results

3.1. Active Components and Related Targets of YXTMD. Using the TCMSP and SwissTarget Prediction databases, the active components of YXTMD were determined, and their related targets were predicted, including for 22 types of renshen, 65 types of danshen, 7 types of guizhi, 22 types of zhishi, and 10 types of zexie. A total of 83 active components and 808 potential related targets were obtained after eliminating compounds without chemical structures or targets and removing repetitive terms.

3.2. Common Targets of "YXTMD-CHD-BSS". Using the GeneCards, OMIM, PharmGkb, TTD, and DrugBank databases, 4003 targets of CHD and 1023 targets of BSS were obtained. Using BioinformaticsGent, 140 common targets were identified at the intersection of "YXTMD-CHD-BSS" (Figure 2).

3.3. "YXTMD Active Components-Common Targets" Network. Perl software was used to sort the data, and 83 active components of YXTMD and 140 common targets were obtained. Using Cytoscape 3.8.2 software, the "YXTMD active components-common targets" network was drawn (Figure 3). The network comprises 223 nodes and 1177 edges. The results showed that the top five components were 5,7,4'-trimethylapigenin (degree = 32), tetramethoxy-luteolin (degree = 31), isosinensetin (degree = 30), sinensetin (degree = 29), and 5,7-dihydroxy-2-(3-hydroxy-4-methoxyphenyl)chroman-4-one (degree = 28) (Table 2).

3.4. "Common Targets" PPI Network. Common targets were imported into the STRING11.5 database to construct the PPI network diagram; isolated nodes were removed

TABLE 1: Primer sequences.

Gene	Sequences (5'→3')	Length (bp)
GAPDH	Forward ACAGCCTCAAGATCATCA GC	104
	Reverse GGTCATGAGTCCTTCCAC GAT	
eNOS	Forward ACCCTCACCGCTACAACA TCC	102
	Reverse TGATTTCCACTGCTGCCT TGTCT	
AKT1	Forward AGCCCTGGACTACCTGCA CTCG	98
	Reverse CTGTGATCTTAATGTGCC CGTCCT	
PI3K	Forward TGCCTACTAAAATGCA TGG	122
	Reverse AACTGAAGGTTAATGGGT CA	
GSK-3β	Forward GCACATCCTTGGACTAAG GTC	229
	Reverse CCAGAGGTGGATTACTTG ACAG	
NF-κB-p65	Forward CGCCTGTCCTTTCATC CCAT	141
	Reverse CCTCTTTCTGCACCTTGT CACAC	

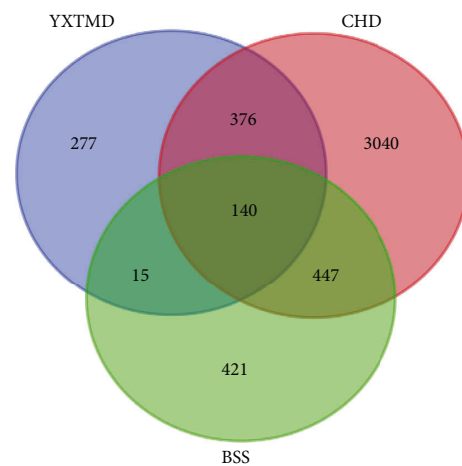


FIGURE 2: Venn diagram showing the common targets of "YXTMD-CHD-BSS."

(Figure 4(a)). The network contained 140 nodes and 677 edges, with an average clustering coefficient of 0.46. We used the Cytoscape plug-in CytoNCA to screen the key genes (Figure 4(b)) and core genes were integrated using two algorithms (Table 3). According to degree size, the order of the core genes was epidermal growth factor receptor (*EGFR*), vascular endothelial growth factor (*VEGF*) A, *AKT1*, *STAT3*, *TP53*, *ERBB2*, *PIK3CA*, *HSP90AA1*, *mTOR*, *SRC*, *CASP3*, matrix metalloproteinase 9 (*MMP9*), *IL2*, *NRAS*, *PTPN11*,

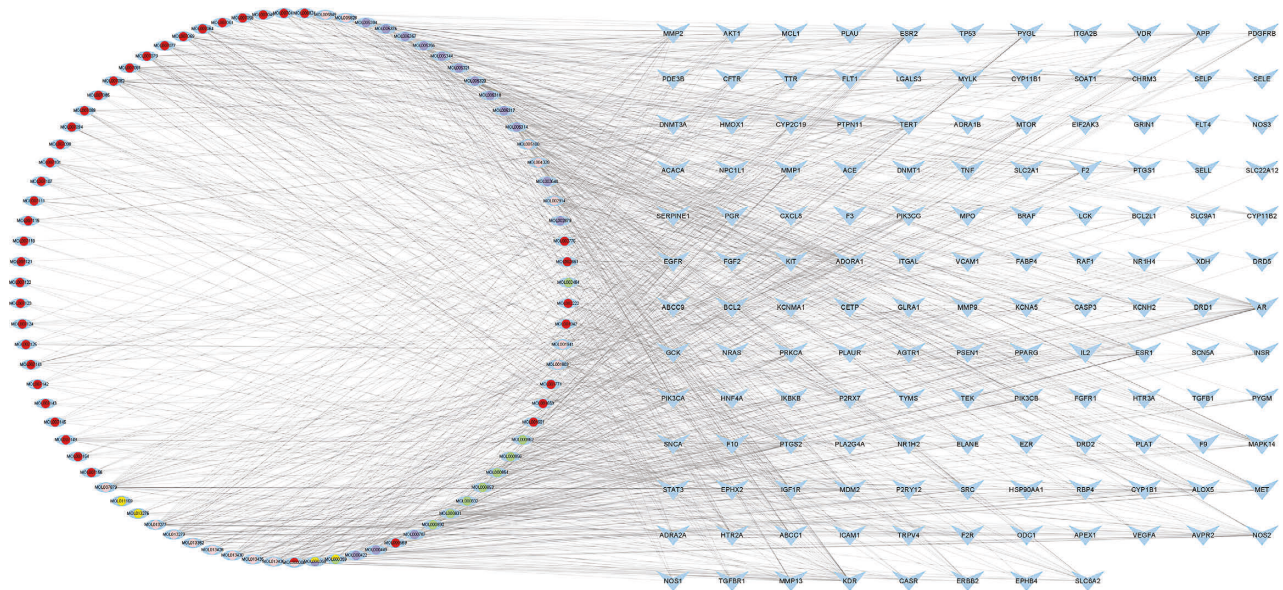


FIGURE 3: “YXTMD active components-common targets” network. Note. The red dots represent danshen, pink dots represent guizhi, yellow dots represent renshen, purple dots represent renshen, and green dots represent zexie. Blue dots represent the common target.

TNF, *PTGS2*, and *FGF2*. These findings indicate that these may be core genes targeted by YXTMD in the treatment of CHD with BSS.

3.5. GO Function and KEGG Enrichment Analyses. In total, 2710 were enriched in the GO analysis, including biological processes (BP), cell composition (CC), and molecular function (MF). The top ten items were selected for visualization (Figure 5). BP was primarily concentrated in wound healing, regulation of body fluid levels, vascular progress in the circulatory system, positive regulation of the MAPK cascade, and positive regulation of kinase activity. CC primarily included the membrane raft, membrane microdomain, plasma membrane raft, caveola, apical part of the cell, and apical plasma membrane. MF was primarily concentrated in transmembrane receptor protein kinase activity, transmembrane receptor protein tyrosine kinase activity, protein tyrosine kinase activity, nuclear receptor activity, and ligand-activated transcription factor activity.

A total of 158 signaling pathways were identified by the KEGG enrichment analysis. The top 30 items were selected for visualization (Figure 6), which primarily included the PI3K-Akt signaling pathway, proteoglycans in cancer, Rap1 signaling pathway, MAPK signaling pathway, microRNAs in cancer, and lipids and atherosclerosis. Based on the network pharmacology results and relevant literature [31], we speculated that the PI3K-Akt signaling pathway was closely related to the treatment of CHD with BSS by YXTMD, and therefore visualized the PI3K-Akt signaling pathway (Figure 7).

3.6. Molecular Docking. Akt1 plays an important role in vascular remodeling, formation, vasodilation, and wound healing by regulating downstream signaling molecules [32]. In addition, VEGF regulates the proliferation of endothelial

cells and promotes angiogenesis through the PI3K-Akt signaling pathway [33]. Accordingly, 5,7,4'-trimethylapigenin, tetramethoxyluteolin, isosinensetin, sinensetin, and 5,7-dihydroxy-2-(3-hydroxy-4-methoxyphenyl)chroman-4-one were selected as the active components for molecular docking with Akt1 and VEGFA (Figure 8).

The results show that the binding energies were less than -5 kcal/mol, indicating that 5,7,4'-trimethylapigenin, tetramethoxyluteolin, isosinensetin, sinensetin, and 5,7-dihydroxy-2-(3-hydroxy-4-methoxyphenyl)chroman-4-one bound strongly to Akt1 and VEGFA (Table 4).

3.7. Clinical Trial Results

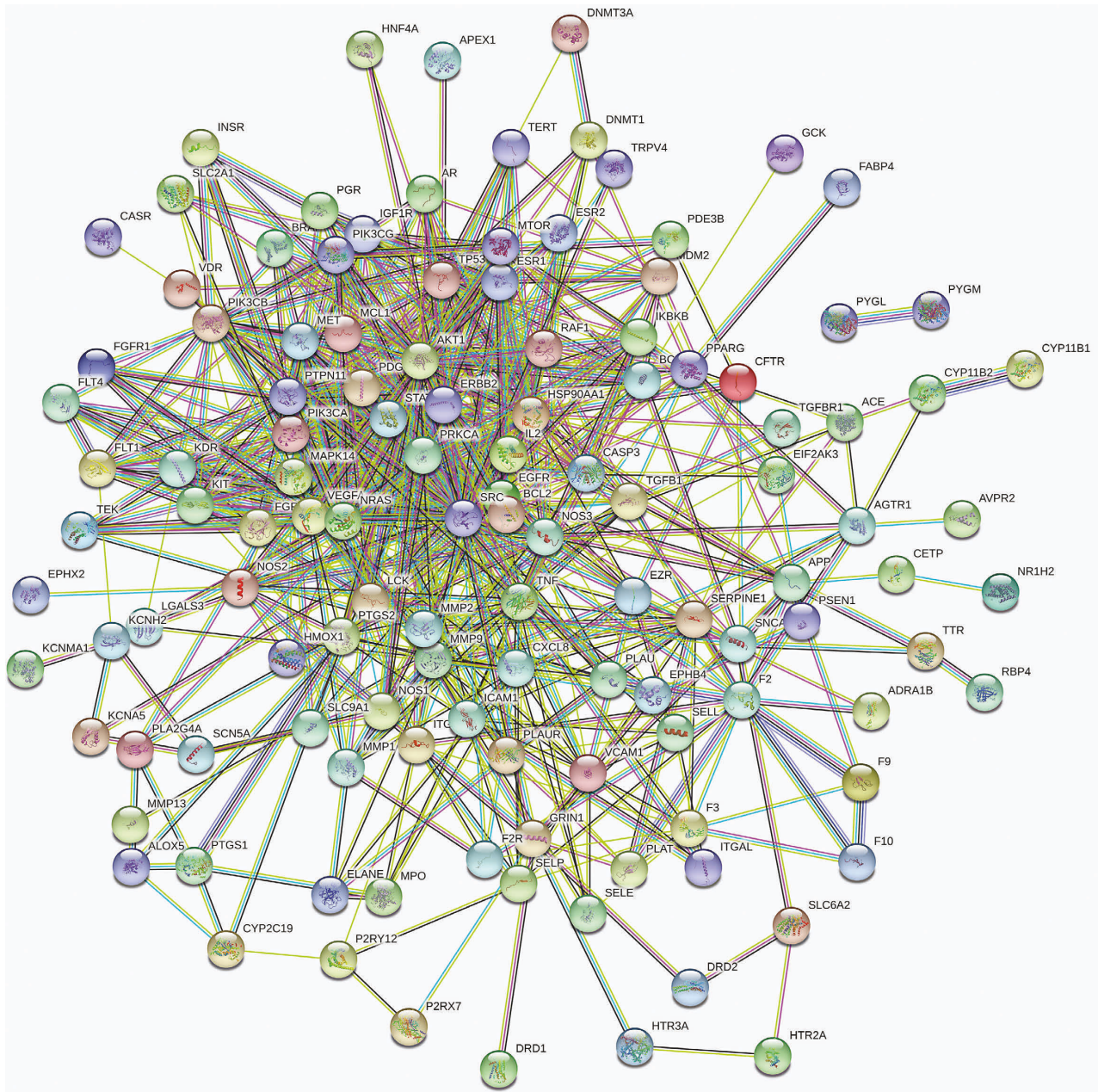
3.7.1. Efficacy of ECG. Those without abnormal ECG before treatment were excluded from the trial. After treatment, the ECG effective rate of the treatment group was 100%, which was higher than that of control group (50%), but the difference was not significant ($P > 0.05$) (Table 5). The small sample size may have impacted these results.

3.7.2. BSS Scores. No statistically significant differences were found between the two groups before treatment, and the data were comparable. Following treatment, the BSS scores decreased in the treatment group ($P < 0.05$). The BSS score also decreased in the control group, but the difference was not significant ($P > 0.05$). The BSS scores of the treatment group showed a more significant decrease compared with those of the control group after treatment ($P < 0.05$) (Table 6).

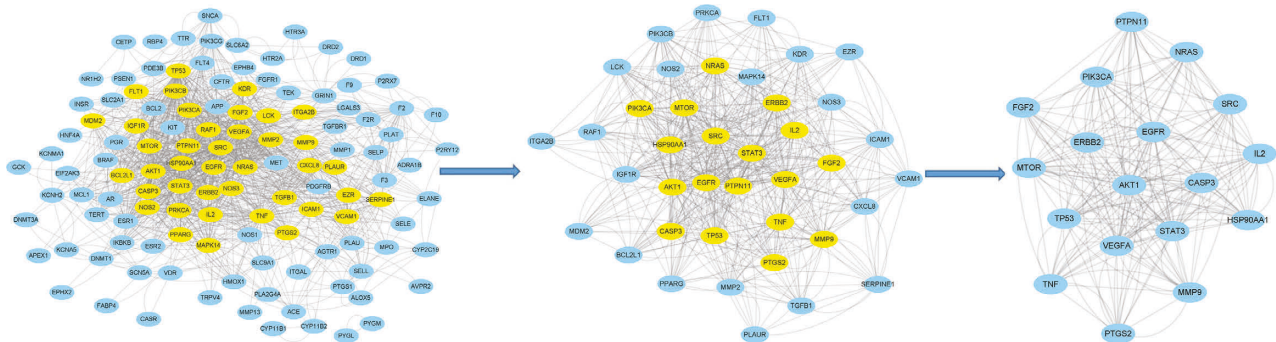
3.7.3. Blood Lipids. No statistically significant differences were found between the two groups before treatment, and the data were comparable. The high-density lipoprotein

TABLE 2: Node degree ranking of main active compounds.

Compound Id	Compound name	Degree	Source
MOL013279	5,7,4'-trimethylapigenin	32	<i>Fructus Aurantii Immaturus</i>
MOL007879	Tetramethoxyluteolin	31	<i>Fructus Aurantii Immaturus</i>
MOL013277	Isosinensetin	30	<i>Fructus Aurantii Immaturus</i>
MOL001803	Sinensetin	29	<i>Fructus Aurantii Immaturus</i>
MOL005100	5,7-dihydroxy-2-(3-hydroxy-4-methoxyphenyl)chroman-4-one	28	<i>Fructus Aurantii Immaturus</i>
MOL007081	Danshenol B	27	<i>Radix Salviae Miltiorrhizae</i>
MOL007082	Danshenol A	27	<i>Radix Salviae Miltiorrhizae</i>
MOL002914	Eriodyctiol (flavanone)	27	<i>Fructus Aurantii Immaturus</i>
MOL000006	Luteolin	26	<i>Radix Salviae Miltiorrhizae</i> and <i>Fructus Aurantii Immaturus</i>
MOL004328	Naringenin	26	<i>Fructus Aurantii Immaturus</i>
MOL000422	Kaempferol	26	<i>Radix Ginseng</i>



(a)



(b)

FIGURE 4: Diagrams of the PPI network and subnetwork topology analysis of common targets. (a) Protein–protein interaction network. (b) Subnetwork topology analysis diagram. Yellow nodes are the core genes obtained after screening.

TABLE 3: Integration of key genes using Degree and CytoNCA algorithms.

Name	Betweenness	Closeness	Degree	Eigenvector	LAC	Network
EGFR	12.49	1.00	34	0.31	21.88	32.46
VEGFA	10.56	0.94	32	0.29	20.75	28.75
AKT1	11.55	0.94	32	0.29	20.25	28.34
STAT3	10.56	0.94	32	0.29	20.75	28.75
TP53	6.63	0.85	28	0.26	19.43	23.71
ERBB2	6.58	0.81	26	0.24	16.92	19.96
PIK3CA	2.16	0.77	24	0.24	18.67	20.35
HSP90AA1	2.56	0.77	24	0.24	18.33	19.81
MTOR	1.80	0.74	22	0.22	17.09	17.90
SRC	2.14	0.74	22	0.22	16.73	17.66
CASP3	2.55	0.74	22	0.21	16.73	18.00
MMP9	2.71	0.74	22	0.21	16.36	17.93
IL2	3.46	0.74	22	0.21	15.64	16.60
NRAS	3.54	0.74	22	0.21	14.91	15.94
PTPN11	1.84	0.71	20	0.20	14.80	15.73
TNF	2.02	0.71	20	0.19	15.20	16.30
PTGS2	0.69	0.68	18	0.18	14.67	15.53
FGF2	2.16	0.68	18	0.18	12.44	13.18

cholesterol (HDL-C) level of the two groups increased after treatment ($P < 0.05$). Total cholesterol (TC), triglyceride (TG), and low-density lipoprotein (LDL) cholesterol (LDL-C) levels were lower in the treatment group, but the difference was not significant ($P > 0.05$); TC and LDL-C levels were higher in the control group ($P < 0.05$). The TC and LDL-C levels of the treatment group showed a greater decrease than those of the after treatment ($P < 0.05$) (Table 7).

3.7.4. Serum Levels of MDA, SOD, NO, IL-1 β , and TNF- α . No statistically significant differences were observed between the two groups before treatment, and the data were comparable. The serum levels of MDA did not significantly change in either group following treatment; the serum levels of SOD and NO were higher in both groups but the difference was not significant ($P > 0.05$). The serum levels of IL-1 β and TNF- α were lower in the treatment group, but the difference was not significant ($P > 0.05$). The serum levels of IL-1 β were significantly higher in the control group ($P < 0.05$), and although the serum levels of TNF- α were also higher, the difference was not significant ($P > 0.05$). Compared with the control group after treatment, no statistical difference was observed in the treatment group (Table 8).

3.7.5. mRNA Levels of PI3k, Akt, NF- κ B, eNOS, and GSK-3 β . No statistically significant differences were found between the two groups before treatment, and the data were comparable. The levels of PI3k, Akt, NF- κ B, and eNOS mRNA were higher in both groups following treatment ($P < 0.05$). The level of GSK-3 β mRNA was significantly lower in the treatment group ($P < 0.05$), and although it was lower in the control group, the difference was not significant ($P > 0.05$). Compared with the control group after treatment, the levels of PI3k and Akt mRNA increased to a greater extent in the treatment group, and the level of GSK-3 β mRNA decreased significantly ($P < 0.05$) (Table 9). Amplification plots and melting curves are shown in Figure 9.

4. Discussion

The pathogenesis of CHD is complex and is primarily related to lipid metabolism disorders, vascular endothelial injury, platelet aggregation, and thrombosis [34]. Disease progression involves the participation of macrophages, smooth muscle cells, endothelial cells, and other cell types [35]. In recent years, researchers have investigated the prevention and treatment of CHD using TCM [36–38]. YXTMD is an effective prescription for the treatment of CHD, and previous studies have confirmed its therapeutic effects. However, the specific active ingredients and mechanisms of action remain unclear. Network pharmacology can be used to effectively integrate TCM and modern medicine, thereby enabling elucidation of the mechanisms of action of TCM compounds at the molecular level. In the present study, a total of 83 active components of YXTMD and 140 “YXTMD-CHD-BSS” common targets were obtained via network pharmacology. Further analysis showed that YXTMD can act on multiple biological functions associated with CHD with BSS and treat the disease via multiple targets, confirming that YXTMD has the hierarchical network characteristics of being “multi-component, multitarget, and multipathway” in the treatment of CHD with BSS.

The results of our study showed that the core active components of YXTMD in the treatment of CHD with BSS were 5,7,4'-trimethylapigenin, tetramethoxyluteolin, isosinensetin, sinensetin, 5,7-dihydroxy-2-(3-hydroxy-4-methoxyphenyl)chroman-4-one, danshenol B, danshenol A, eriodictiol, luteolin, naringenin, and kaempferol. The first 10 components belonged to danshen and zhishi. Danshen (*Radix Salviae Miltiorrhizae*) activates the blood and resolves stasis, and zhishi (*Fructus Aurantii Immaturus*) regulates qi and dissipates phlegm, consistent with the principle of treating BSS. Most of the active ingredients were flavonoids, which have the effects of antioxidation, anti-inflammation, vasodilation, inhibition of platelet aggregation, and regulation of blood lipid levels, thus exerting beneficial

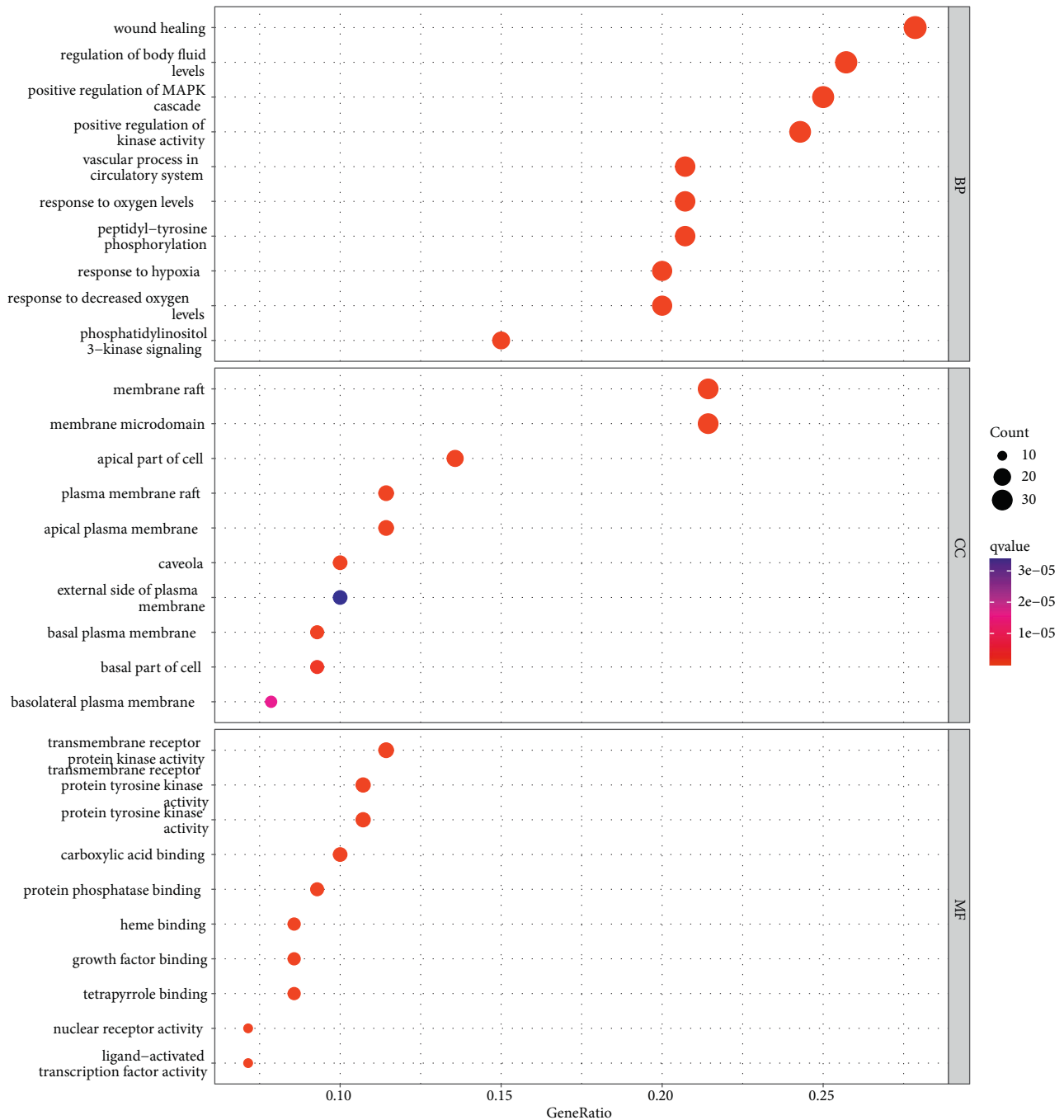


FIGURE 5: GO functional analysis.

therapeutic effects on cardiovascular and cerebrovascular diseases [39–41]. Modern research has shown that sinensetin can exert various pharmacological effects, including anti-inflammatory and antioxidant effects, by reducing the secretion of inflammatory factors such as IL-1 β , IL-6, and TNF- α [42]. In addition, 5,7-dihydroxy-2-(3-hydroxy-4-methoxyphenyl)chroman-4-one can scavenge oxygen-free radicals and has anti-inflammatory and blood lipid-lowering effects [43]. Danshenol effectively inhibits calcium overload in tissues, thereby reducing myocardial ischemia injury in rats [44]. Luteolin can scavenge reactive

oxygen species and reduce oxidative damage in inflammatory cells [45]. It can also regulate inflammatory mediators and inflammatory factors, affecting the cyclooxygenase and lipoxygenase pathways to affect the arachidonic acid pathway, thereby reducing the production of prostaglandins to protect the cardiovascular system and inhibit platelet activity and arterial thrombosis [46]. Naringenin has antioxidant, anti-inflammatory, and anti-apoptotic effects [47] and can also inhibit platelet activity and arterial thrombosis [48]. Kaempferol plays an important role in the inflammatory response and can reduce the

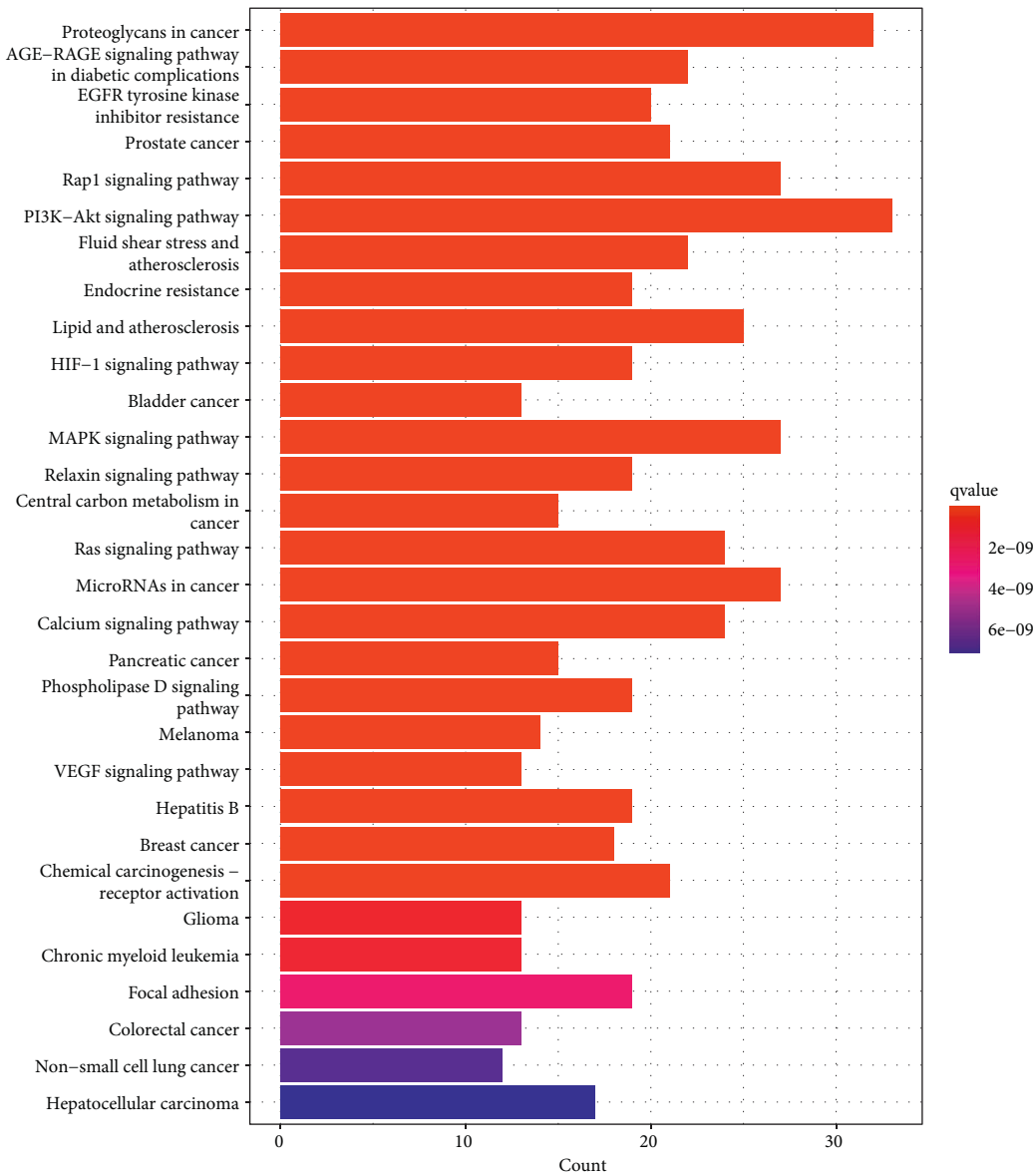


FIGURE 6: KEGG enrichment analysis.

expression of reduced coenzyme oxidase to inhibit ROS generation, protect protein tyrosine phosphatase-2 (SHP-2), and inhibit platelet activation. It can also prevent CHD as well as other cardiovascular and cerebrovascular diseases [49]. This suggests that YXTMD can treat CHD with BSS by exerting anti-inflammatory, antioxidation, and antithrombotic effects, and regulating lipid metabolism. In this compound, danshen and zhishi are the main drugs that show efficacy and should be considered as important directions for later drug development.

In the present study, we identified 18 key targets of YXTMD for the treatment of CHD with BSS: EGFR, VEGFA, AKT1, STAT3, TP53, ERBB2, PIK3CA, HSP90AA1, MTOR, SRC, CASP3, MMP9, IL2, NRAS, PTPN11, TNF, PTGS2, and FGF2. Previous studies have shown that VEGFA, EGFR, and FGF2 are related to vascular endothelial regeneration, and that vascular endothelial cell

damage is a significant feature of atherosclerosis [50]. VEGF can act on vascular endothelial cells and regulate endothelial cell proliferation through the PI3K-Akt signaling pathway, thereby promoting angiogenesis [33]. EGFR is involved in the vascular pathophysiology and oxidative stress of macrophages, and inhibition of EGFR can resist oxidative stress, macrophage infiltration, and proliferation of SMCs in lesions [51]. FGF2 regulates cell differentiation and proliferation and promotes the angiogenic activity of human microvascular endothelial cells [52]. AKT1 is a serine/threonine protein kinase that controls the cell cycle, protein synthesis, and angiogenesis [53]. Akt can regulate various downstream signaling molecules, such as eNOS, which plays an important role in vascular remodeling and relaxation, angiogenesis, and wound healing [32]. Inhibition of the transcription factor STAT3 can mediate increased M2 phenotypic differentiation of macrophages, thereby

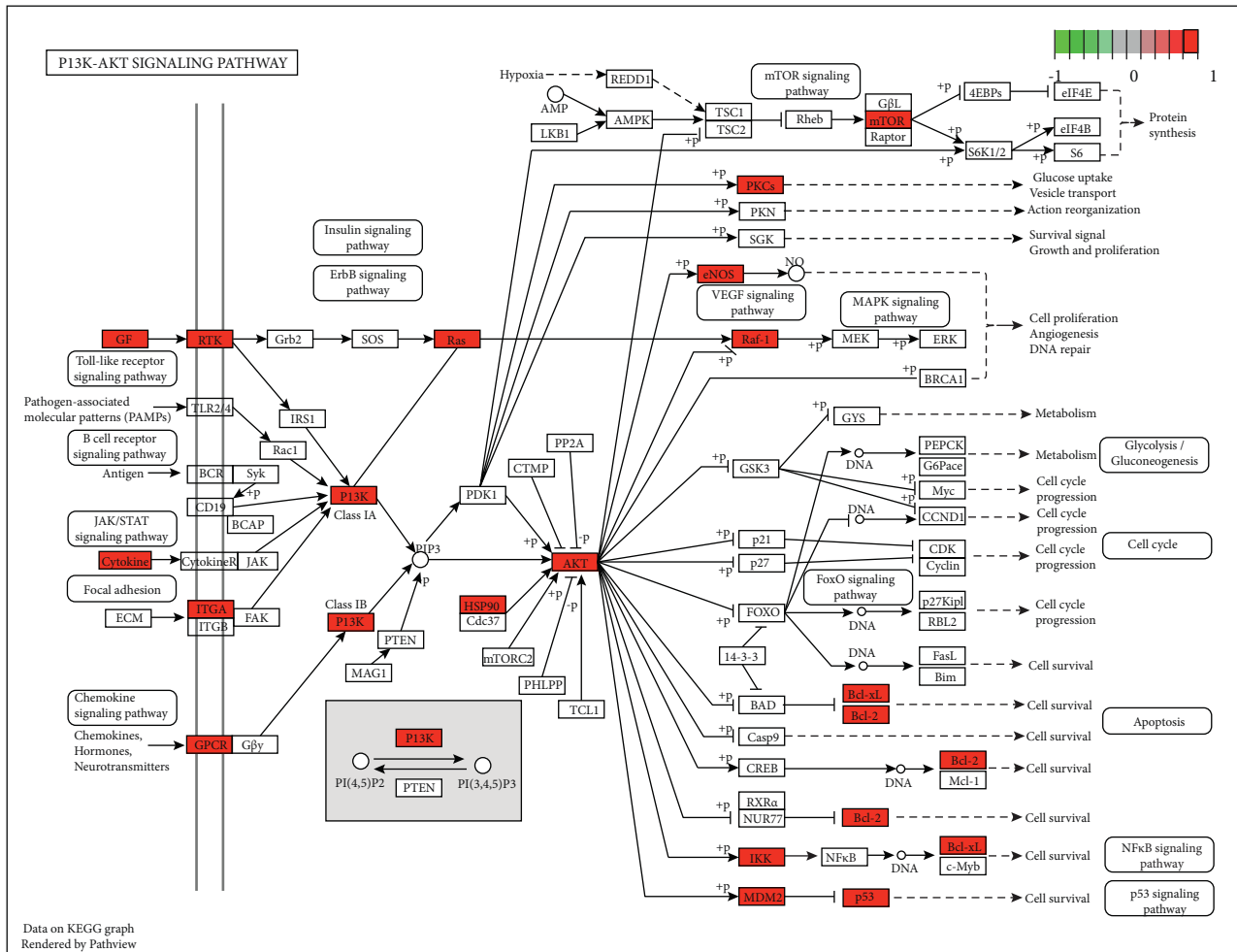


FIGURE 7: Visualization of the PI3K-Akt signaling pathway.

inhibiting the formation of atherosclerotic plaques [54]. TP53 is a tumor suppressor protein that plays a role in atherosclerosis development as well as the growth and death of vascular smooth muscle cells by regulating cellular senescence, proliferation, and apoptosis [55]. ERBB2 is a tyrosine kinase receptor, and a previous study showed that activation of the NRG-ERBB pathway can promote the regeneration of cardiomyocytes, thereby repairing damaged myocardial function [56]. The mTOR protein is a serine/threonine protein kinase downstream of PI3K-Akt that is involved in regulating cell survival, apoptosis, and proliferation [57]. SRC is involved in various biological processes including cell proliferation, movement, and migration. It can activate the phosphorylation of the Y357 site on yes-related proteins, thereby regulating the Gp130 protein to promote cardiomyocyte proliferation during cardiac regeneration [58]. CASP3 is the initiator and executor of apoptosis. A previous study has shown that CASP3 can regulate oxidative stress damage to a certain extent, thereby reducing myocardial damage [59]. Moreover, TNF, IL2, MMP9, and PTGS2 play important roles in the inflammatory response. TNF is a tumor necrosis factor that can also promote atherosclerosis by increasing the

endocytosis of LDL in endothelial cells, thereby promoting the deposition of LDL in the vascular walls [60]. IL2 is an inflammatory factor that is related to the formation of atherosclerosis. MMP9 is a matrix metalloproteinase that is involved in various pathological processes, such as inflammation and atherosclerosis. PTGS2 converts arachidonic acid to prostaglandins and is overexpressed under mechanical, chemical, and physical stimulation, thereby promoting the development of an inflammatory response. The molecular docking results of this study also showed that the core active components of YXTMD could bind well to the key targets AKT1 and VEGFA, which can be used as important indicators for future research.

In the present study, GO functional and KEGG enrichment analyses revealed that YXTMD primarily targets the PI3K-Akt signaling pathway, proteoglycan in cancer, Rap1 signaling pathway, MAPK signaling pathway, microRNAs in cancer, and lipids and atherosclerosis in the treatment of CHD with BSS. The primary biological processes involved included wound healing, regulation of body fluid levels, and vascular progress in the circulatory system. The PI3K-Akt pathway plays an important role in growth in vivo, and can activate antiapoptotic mechanisms, glucose

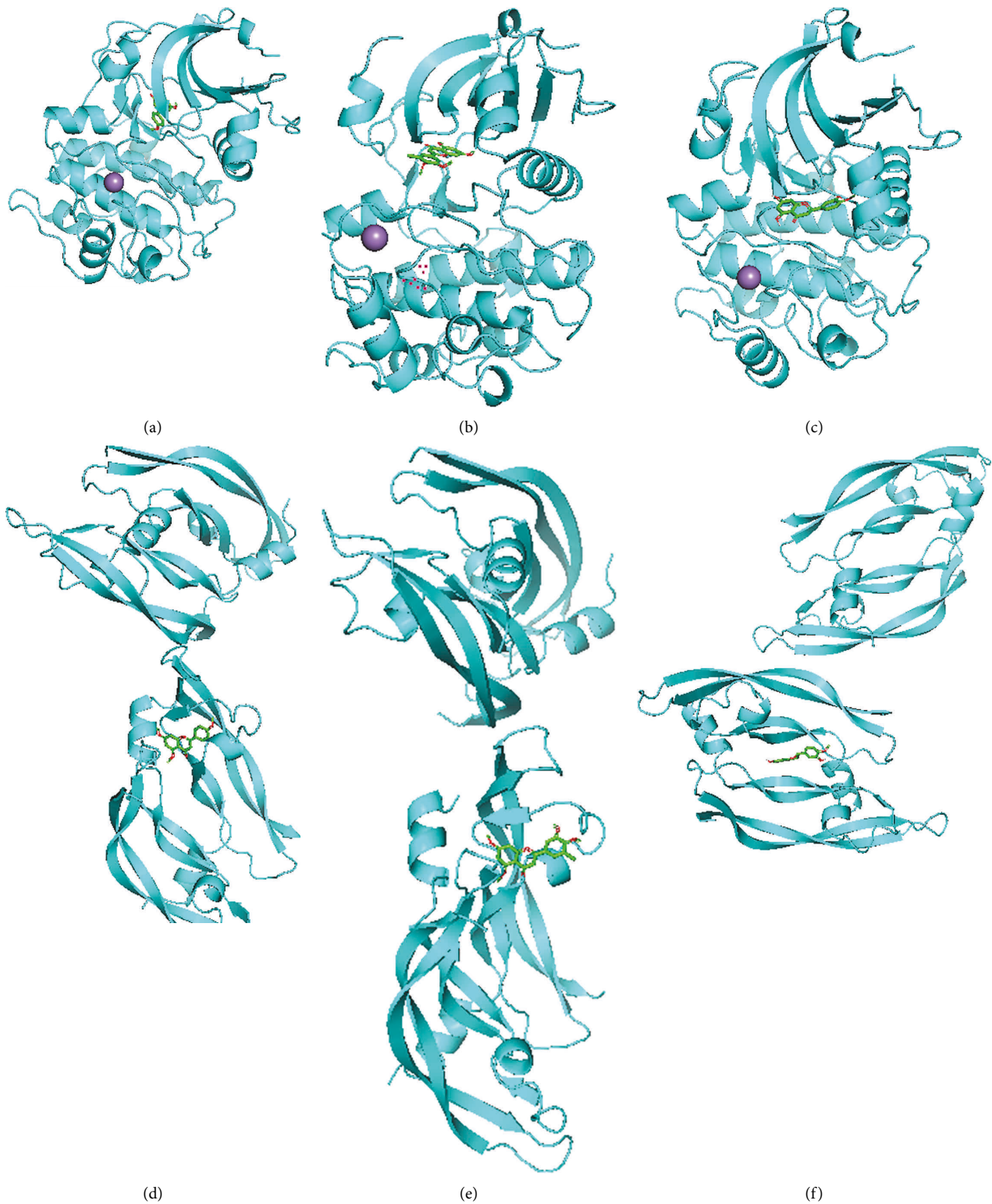


FIGURE 8: Results of molecular docking. Structures show molecular docking of (a) AKT1-5,7,4'-trimethylapigenin, (b) AKT1-tetramethoxyluteolin, (c) AKT1-5,7-dihydroxy-2-(3-hydroxy-4-methoxyphenyl)chroman-4-one, (d) VEGFA-5,7,4'-trimethylapigenin, (e) VEGFA-tetramethoxyluteolin, and (f) VEGFA-5,7-dihydroxy-2-(3-hydroxy-4-methoxyphenyl)chroman-4-one.

metabolism, protein synthesis, and other processes to promote cell proliferation [61]. It also plays an important role in the regulation of cardiomyocytes, survival, and

function [62]. The PI3K-Akt pathway can also regulate the inflammatory response and oxidative stress injury, which are closely related to the formation of atherosclerosis [63]. AKT1

TABLE 4: Molecular docking (unit: kcal/mol).

Number	Molecule name	Molecular formula	AKT1	VEGFA
1	5,7,4'-trimethylapigenin	C18H16O5	-8.5	-6.8
2	Tetramethoxyluteolin	C19H18O6	-8.8	-6.7
3	Isosinensetin	C20H20O7	-8.2	-6.8
4	Sinensetin	C20H20O7	-8.1	-6.3
5	5,7-dihydroxy-2-(3-hydroxy-4-methoxyphenyl)chroman-4-one	C16H14O6	-8.5	-7.1

TABLE 5: Comparison of ECG effective rate between the two groups (%).

Groups	N	Markedly effective	Effective	Ineffective	Total effective rate (%)
Treatment group	4	2 (50)	2 (50)	0 (0)	100
Control group	6	1 (16.7)	2 (33.3)	3 (50)	50

TABLE 6: Comparison of blood stasis syndrome scores between the two groups ($\bar{x} \pm s$).

Groups	N	Before treatment	After treatment	P value
Treatment group	7	35.71 \pm 9.09	19.29 \pm 7.30	<0.05*
Control group	7	31.71 \pm 8.83	27.43 \pm 10.08	0.182
P Value		0.396	<0.05 [#]	

Note. * $P < 0.05$ compared to pretreatment; [#] $P < 0.05$ compared to the control group after treatment.

TABLE 7: Comparison of blood lipids before and after treatment between the two groups ($\bar{x} \pm s$, $n = 7$).

Items	Treatment group		Control group	
	Before treatment	After treatment	Before treatment	After treatment
TC	3.63 \pm 1.07	3.41 \pm 0.81 [#]	3.82 \pm 0.69	4.38 \pm 0.51*
TG	1.41 \pm 0.68	1.33 \pm 0.60	2.24 \pm 1.28	1.88 \pm 0.83
LDL-C	2.50 \pm 0.97	2.14 \pm 0.78 [#]	2.54 \pm 0.54	2.99 \pm 0.48*
HDL-C	0.97 \pm 0.29	1.11 \pm 0.27*	0.99 \pm 0.27	1.21 \pm 0.33*

Note. * $P < 0.05$ compared to pretreatment; [#] $P < 0.05$ compared to the control group after treatment.

TABLE 8: Comparison of serum levels of MDA, SOD, NO, TNF- α , and IL-1 β before and after treatment between the two groups ($\bar{x} \pm s$, $n = 7$).

Items	Treatment group		Control group	
	Before treatment	After treatment	Before treatment	After treatment
MDA	0.11 \pm 0.01	0.11 \pm 0.01	0.12 \pm 0.01	0.13 \pm 0.01
SOD	0.20 \pm 0.06	0.25 \pm 0.05	0.19 \pm 0.03	0.22 \pm 0.02
NO	4.89 \pm 1.91	6.10 \pm 2.57	6.13 \pm 2.81	7.93 \pm 2.53
IL-1 β	15.76 \pm 3.92	12.57 \pm 4.04	15.50 \pm 2.79	18.60 \pm 2.86*
TNF- α	16.66 \pm 2.19	16.30 \pm 0.99	18.57 \pm 3.17	19.30 \pm 2.91

Note. * $P < 0.05$ Compared to pretreatment.

TABLE 9: Comparison of the levels of PI3k, Akt, NF- κ B, eNOS, and GSK-3 β mRNA before and after treatment between the two groups ($\bar{x} \pm s$, $n = 7$).

Items	Treatment group		Control group	
	Before treatment	After treatment	Before treatment	After treatment
PI3k	1.43 \pm 0.85	3.03 \pm 0.38 [#]	1.04 \pm 0.49	1.70 \pm 0.72*
Akt	1.05 \pm 0.33	3.43 \pm 1.04 [#]	1.16 \pm 0.77	2.20 \pm 0.81*
NF- κ B	0.90 \pm 0.42	2.51 \pm 0.85*	0.99 \pm 0.43	1.85 \pm 0.73*
eNOS	0.80 \pm 0.21	1.76 \pm 0.58*	0.86 \pm 0.29	1.32 \pm 0.41*
GSK-3 β	1.34 \pm 0.35	0.35 \pm 0.94 [#]	1.07 \pm 0.39	0.80 \pm 0.29

Note. * $P < 0.05$ compared to pretreatment; [#] $P < 0.05$ compared to the control group after treatment.

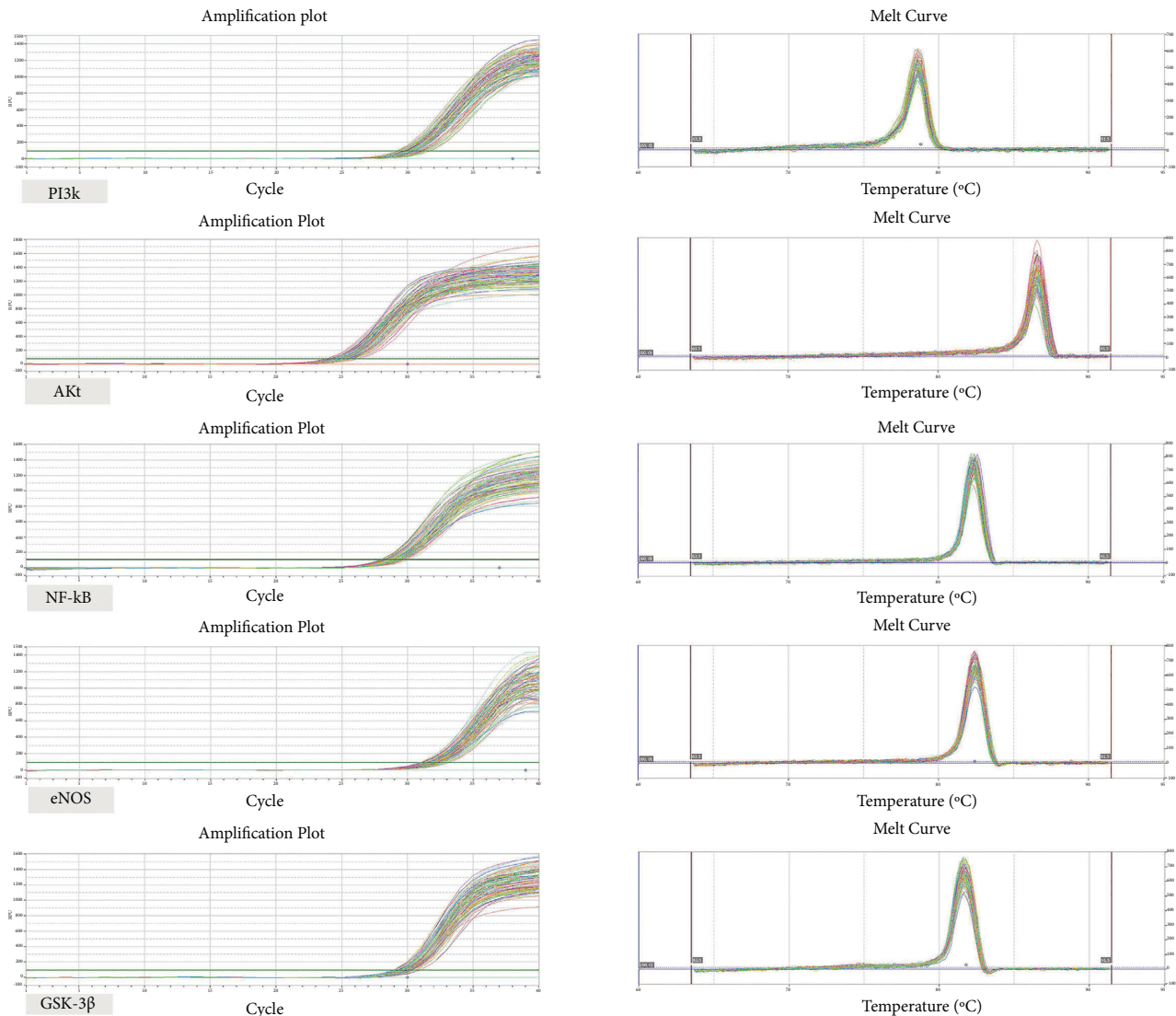


FIGURE 9: Amplification plots and melting curves.

is the center of the PI3K-Akt signaling pathway, and inhibition of its overactivation can alleviate high-fat-diet-induced atherosclerosis in ApoE + mice [64]. It participates in various biological processes, such as cell metabolism, proliferation, and survival, by regulating various downstream signaling molecules [65]. The downstream targets of the PI3K-Akt pathway include eNOS, NF- κ B, and GSK-3 β . Activated Akt can phosphorylate eNOS, thereby promoting the production of endogenous NO, accelerating the regeneration of vascular endothelial cells, and dilating blood vessels. NF- κ B promotes cell proliferation, inhibits apoptosis, and is an important inflammatory activator [66]. GSK-3 β is a multifunctional serine/threonine protein kinase that negatively regulates itself by activating the PI3K-Akt pathway, thereby mediating cell metabolism, proliferation, differentiation, apoptosis, and other biological processes [67]. Accordingly, regulation of these target molecules can promote the regeneration of vascular endothelial cells, reduce inflammation, resist oxidative stress, and regulate

carbohydrate and lipid metabolism. Based on these results, we speculated that the PI3K-Akt pathway was closely related to the treatment of CHD with BSS by YXTMD.

Based on previous research from our group and the pathogenesis of CHD with BSS, we further verified the accuracy of the network pharmacology results and more intuitively reflected the clinical efficacy and specific molecular mechanism of YXTMD in the treatment of CHD with BSS through a clinical trial. In the trial, we determined the effects of the clinical efficacy, blood lipid level, endothelial injury marker index (NO), inflammatory factor index (IL-1 β and TNF- α), oxidative stress indicators (MDA and SOD), and the PI3K-Akt pathway and its downstream proteins (PI3k, AKt, NF- κ B, eNOS, and GSK-3 β) in patients with CHD with BSS. Results showed that after treatment, the clinical curative effect of the treatment group was better than that of the control group. YXTMD improved the curative effect scores of patients with BSS and reduced the serum TC and LDL-C levels. PCR results showed that, compared with

the control group, the serum levels of PI3k and AKt mRNA significantly increased, and the levels of GSK-3 β mRNA significantly decreased in the treatment group; however, the levels of *NF- κ B* and *eNOS* mRNA did not significantly change. ELISA results showed no significant changes in serum MDA, SOD, NO, and TNF- α levels in the two groups before and after treatment, and the serum IL-1 β level in the control group was higher than before treatment. The above results demonstrate that YXTMD was clinically effective in treating CHD with BSS. It can improve the efficacy score of BSS and reduce blood lipid levels. The specific mechanism may be related to the activation of the PI3K/Akt signaling pathway, downregulation of GSK-3 β , and regulation of lipid metabolism.

Notably, this study has some limitations. Preliminary research results showed that the main active components of YXTMD have anti-inflammatory, antioxidant, vasodilatory, antithrombotic, and lipid-metabolism-regulating effects. However, the results of later clinical trials have revealed that YXTMD activates the PI3K/Akt signaling pathway and is primarily involved in regulating lipid metabolism. Its anti-inflammatory, antioxidant, and vasodilatory effects were not obvious, which may be explained by the following factors: (1) This trial was based on a heterogeneous human population, which involves many uncontrollable factors. (2) The difficulty in collecting clinical samples and the problem of patient compliance resulted in a small sample size. (3) The subjects of this study were all patients with BSS. Modern studies have shown that increased blood lipids and viscosity are the biochemical basis for phlegm and blood stasis. This occurs when a large amount of lipids condense in the veins to form phlegm turbidity, and the phlegm is stuck in the veins for a prolonged period and condenses into blocks, leading to endogenous blood stasis. Therefore, BSS formation was closely related to blood lipid levels. These factors affected the trial results to some extent, so large-scale clinical studies or in-depth studies at the animal and cellular levels are needed at a later stage to explore the specific mechanism by which YXTMD treats CHD with BSS.

5. Conclusions

Our study explored the mechanism of action of YXTMD in the treatment of CHD with BSS through a combination of network pharmacology and molecular docking. The results demonstrated that 5,7,4'-trimethoxyflavone, tetramethoxyluteolin, isosinensetin, sinensetin, and 5,7-dihydroxy-2-(3-hydroxy-4-methoxyphenyl)chroman-4-one may be the main active components of YXTMD. These components act on key targets, such as EGFR, VEGFA, AKT1, STAT3, TP53, ERBB2, and PIK3CA, in the treatment of CHD with BSS. YXTMD had the characteristics of being multicomponent, multitarget, and multipathway in treating CHD with BSS. Clinical trial results showed that the mechanism of action of YXTMD in treating CHD with BSS may be related to the activation of the PI3K-Akt signaling pathway, downregulation of GSK-3 β , and mediation of lipid-metabolism-based metabolic processes. These results provide a theoretical basis for the clinical application of YXTMD and

highlight directions for follow-up studies on the development of anti-CHD drugs.

Data Availability

All data obtained or analyzed during this study are included within the article.

Disclosure

Mengxue Zhang and Jia Liu are the co-first authors.

Conflicts of Interest

The authors declare that they have no conflicts of interest.

Authors' Contributions

Jie Li and Lingli Chen designed the study, coordinated technical support and funding; Mengxue Zhang and Jia Liu contributed equally to this paper, they finished the study, analyzed the data, and wrote the manuscript; Xiangzhuo Zhang, Shumeng Zhang, Yujie Jiang, Zixuan Yu, Ting Xie, and Yuxia Chen participated in the study. All authors read and approved the final manuscript.

Acknowledgments

This study was supported by the National Natural Science Foundation of China (Grant No. 81874375), Natural Science Foundation of Hunan Province, China (Grant No. 2020JJ4464), Key project of Traditional Chinese Medicine Research Program of Hunan Province (Grant No. 2021024), and Key Research Program project of Hunan University of Traditional Chinese Medicine (Grant No. 2020XJJ002).

References

- [1] T. T. Wang, B. Dong, and D. H. Wang, "Discussion on Yangxin Tongmai ointment "harmonize Qixue and Yinyang" in the treatment of chest obstruction and heart pain," *Chinese Journal of Integrative Medicine on Cardio-/Cerebrovascular Disease*, no. 2, pp. 246-247, 2018.
- [2] G. A. Roth, G. A. Mensah, and V. Fuster, "The global burden of cardiovascular diseases and risks: a compass for global action," *Journal of the American College of Cardiology*, vol. 76, no. 25, pp. 2980-2981, 2020.
- [3] S. S. Virani, A. Alonso, H. J. Aparicio et al., "Heart disease and stroke statistics-2021 update: a report from the American heart association," *Circulation*, vol. 143, no. 8, pp. e254-e743, 2021.
- [4] "Guidelines for rational drug use in coronary heart disease (2nd Edition)," *Chinese Journal of Forensic Medicine*, vol. 10, no. 6, pp. 1-130, 2018.
- [5] M. Gimbel, K. Qaderdan, L. Willemsen et al., "Clopidogrel versus ticagrelor or prasugrel in patients aged 70 years or older with non-ST-elevation acute coronary syndrome (POPular AGE): the randomised, open-label, non-inferiority trial," *Lancet*, vol. 395, no. 10233, pp. 1374-1381, 2020.
- [6] H. Bays, D. E. Cohen, N. Chalasani, S. A. Harrison, and The National Lipid Association's Statin Safety Task Force, "An assessment by the statin liver safety task force: 2014 update,"

- Journal of Clinical Lipidology*, vol. 8, no. 3 Suppl, pp. S47–S57, 2014.
- [7] M. M. Rahman, M. R. Islam, S. Shohag et al., “The multi-functional role of herbal products in the management of diabetes and obesity: a comprehensive review,” *Molecules*, vol. 27, no. 5, p. 1713, 2022.
- [8] A. Akter, F. Islam, S. Bepary et al., “CNS depressant activities of Averrhoa carambola leaves extract in thio-pental-sodium model of Swiss albino mice: implication for neuro-modulatory properties,” *Biologia*, vol. 77, 2022.
- [9] K. J. Zhang, Q. Zheng, P. C. Zhu et al., “Traditional Chinese medicine for coronary heart disease: clinical evidence and possible mechanisms,” *Frontiers in Pharmacology*, vol. 10, p. 84, 2019.
- [10] D.-C. Fan, J.-Y. Qi, and M.-Z. Zhang, “Insights of Chinese medicine on ventricular remodeling: multiple-targets, individualized-treatment,” *Chinese Journal of Integrative Medicine*, vol. 23, no. 9, pp. 643–647, 2017.
- [11] M. M. Rahman, P. S. Dhar, Sumaia et al., “Exploring the plant-derived bioactive substances as antidiabetic agent: an extensive review,” *Biomedicine & Pharmacotherapy*, vol. 152, Article ID 113217, 2022.
- [12] S.-H. Luo, Y. Li, L.-J. Zhao et al., “Distribution characteristics of traditional Chinese medicine syndromes in patients with critical lesions of coronary heart disease,” *Chinese Journal of Experimental Traditional*, vol. 26, no. 9, pp. 53–57, 2020.
- [13] B. W. Qin, *Qianzhai Medical Lecture*, Shanghai Science and Technology publish, Shanghai, China, 1978.
- [14] X.-M. Zhou, “Clinical observation of Treating angina of qiynliangxu with blood stasis in the recipe of Yangxin Tongmai,” *Clinical Journal of Chinese Medicine*, vol. 42, no. 2, p. 2021, 2012.
- [15] Q.-H. Chen, M. Li, and Z.-K. Yuan, “Experimental study of Yangxin Tongmai recipe effective component parts anti-acute myocardial ischemia,” *Chinese Archives of Traditional Chinese Medicine*, vol. 26, no. 9, pp. 1910–1913, 2008.
- [16] M.-L. Zhou, Y.-F. Yu, X.-X. Luo et al., “LC-MS-Based metabonomics study of Yangxin tongmaifang against coronary heart disease differentiated into blood stasis syndrome,” *Chinese Journal of Experimental Traditional*, vol. 27, no. 22, pp. 139–146, 2021.
- [17] J. L. Ru, *Construction and Utilization of Traditional Chinese Medicine Systems Pharmacology Database and Analysis Platform*, Northwest A&F University, Yangling, China, 2015.
- [18] S. Tian, Y. Li, J. Wang, J. Zhang, and T. Hou, “ADME evaluation in drug discovery. 9. Prediction of oral bio-availability in humans based on molecular properties and structural fingerprints,” *Molecular Pharmaceutics*, vol. 8, no. 3, pp. 841–851, 2011.
- [19] S. Tian, J. Wang, Y. Li, X. Xu, and T. Hou, “Drug-likeness analysis of traditional Chinese medicines: prediction of drug-likeness using machine learning approaches,” *Molecular Pharmaceutics*, vol. 9, no. 10, pp. 2875–2886, 2012.
- [20] S. Kim, J. Chen, T. Cheng et al., “PubChem 2019 update: improved access to chemical data,” *Nucleic Acids Research*, vol. 47, no. D1, pp. D1102–D1109, 2019.
- [21] D. Gfeller, O. Michielin, and V. Zoete, “Shaping the interaction landscape of bioactive molecules,” *Bioinformatics*, vol. 29, no. 23, pp. 3073–3079, 2013.
- [22] C. von Mering, L. J. Jensen, B. Snel et al., “STRING: known and predicted protein-protein associations, integrated and transferred across organisms,” *Nucleic Acids Research*, vol. 33, pp. D433–D437, 2005.
- [23] D. Szklarczyk, A. L. Gable, D. Lyon et al., “STRING v11: protein-protein association networks with increased coverage, supporting functional discovery in genome-wide experimental datasets,” *Nucleic Acids Research*, vol. 47, no. D1, pp. D607–D613, 2019.
- [24] C. Feng, M. Zhao, L. Jiang, Z. Hu, and X. Fan, “Mechanism of modified danggui sini decoction for knee osteoarthritis based on network pharmacology and molecular docking,” *Evid Based Complement Alternat Med*, vol. 2021, Article ID 6680637, 11 pages, 2021.
- [25] O. Trott, A. J. Olson, and A. D. Vina, “Improving the speed and accuracy of docking with a new scoring function, efficient optimization, and multithreading,” *Journal of Computational Chemistry*, vol. 31, no. 2, pp. 455–461, 2010.
- [26] Chinese Society of Cardiology and Chinese Medical Association; Editorial Board, “Guideline for diagnosis and treatment of patients with chronic stable angina,” *Chinese Journal of Cardiology*, vol. 35, no. 03, pp. 195–206, 2007.
- [27] Y.-N. Ke and J.-L. Chen, “Guideline for diagnosis and treatment of patients with unstable angina and non-ST-segment elevation myocardial infarction,” *Chinese Journal of Cardiology*, vol. 35, no. 04, pp. 295–304, 2007.
- [28] K. J. Chen, D. Z. Shi, and C. G. Fu, “Diagnostic criteria of coronary heart disease with blood stasis syndrome,” *Chinese Journal of Integrated Traditional and Western Medicine*, vol. 36, no. 10, p. 1162, 2016.
- [29] J.-L. Chen, “Evaluation criteria for angina pectoris and electrocardiogram in coronary heart disease,” *People’s Military Surgeon*, vol. 5, p. 62, 1974.
- [30] J. Wang and Q.-Y. He, “Evaluation criteria of angina pectoris and blood stasis in coronary heart disease,” *Chinese Journal of Experimental Traditional Medical Formulae*, vol. 24, no. 15, pp. 1–3, 2018.
- [31] Q. Lin, *Study on the Mechanism of the Compatibility of American Ginseng and Salvia Miltiorrhiza in Regulating PI3K/Akt/NF- κ B Pathway to Stabilize Atherosclerotic Vulnerable Plaques*, China Academy of Chinese Medical Sciences, Beijing, China, 2021.
- [32] Q. Chen, T. Xu, D. Li et al., “JNK/PI3K/Akt signaling pathway is involved in myocardial ischemia/reperfusion injury in diabetic rats: effects of salvianolic acid A intervention,” *American Journal of Tourism Research*, vol. 8, no. 6, pp. 2534–2548, 2016.
- [33] J.-X. Zhou, L. Chen, and B.-C. Chen, “Vascular endothelial growth factor promotes angiogenesis in cerebral infarction rats through PI3K-Akt and MAPK-ERK pathways,” *Chinese Journal of Gerontology*, vol. 39, no. 15, pp. 3749–3752, 2019.
- [34] “Experts consensus on prevention and treatment of atherosclerosis by integrative medicine(2021),” *Chinese Journal of Integrated Traditional and Western Medicine*, vol. 42, no. 03, pp. 287–293, 2022.
- [35] G. Machado-Oliveira, C. Ramos, A. Marques, and O. V. Vieira, “Cell senescence, multiple organelle dysfunction and atherosclerosis,” *Cells*, vol. 9, no. 10, pp. 21–46, 2020.
- [36] X.-F. Li, Y. Fu, and J.-D. Zhou, “Effects and the mechanism of trichosanthes pericarpium on endothelial progenitor cells mobilization in acute myocardial ischemia rats,” *China Journal of Traditional Chinese Medicine and Pharmacy*, vol. 34, no. 03, pp. 1210–1214, 2019.
- [37] J. Wang, “To study the effect of xuefu zhuyu decoction on blood lipid, serum inflammatory factors and endothelial function in patients with coronary heart disease,” *Guide of China Medicine*, vol. 18, no. 19, pp. 160–161, 2020.

- [38] T. Zhou, K.-D. Ning, and Z.-S. Li, "The regulatory effect of Taohong Siwu decoction on the level of blood lipid in atherosclerotic rats," *China Medicine and Pharmacy*, vol. 10, no. 17, pp. 36–38, 2020.
- [39] X.-G. Li, L.-H. Fang, and G.-H. Du, "Research progress on cardiovascular protective mechanism of flavonoids," *Chinese Pharmacological Bulletin*, vol. 34, no. 6, p. 741, 2018.
- [40] M. M. Rahman, M. S. Rahaman, M. R. Islam et al., "Role of phenolic compounds in human disease: current knowledge and future prospects," *Molecules*, vol. 27, no. 1, pp. 23–33, 2021.
- [41] S. Mitra, M. S. Lami, T. M. Uddin et al., "Prospective multifunctional roles and pharmacological potential of dietary flavonoid narirutin," *Biomedicine & Pharmacotherapy*, vol. 150, pp. 1129–1132, 2022.
- [42] J. L. Han, I. Jantan, S. D. Yusoff, J. Jalil, K. Husain, and Sinensetin, "An insight on its pharmacological activities, mechanisms of action and toxicity," *Frontiers in Pharmacology*, vol. 11, Article ID 553404, 2020.
- [43] F. Islam, J. F. Khadija, M. Harun-Or-Rashid et al., "Bioactive compounds and their derivatives: an insight into prospective phytotherapeutic approach against alzheimer's disease," *Oxidative Medicine and Cellular Longevity*, vol. 2022, Article ID 5100904, 22 pages, 2022.
- [44] F. Liu, Z. Z. Huang, Y. H. Sun et al., "Four main active ingredients derived from a traditional Chinese medicine guanxin shutong capsule cause cardioprotection during myocardial ischemia injury calcium overload suppression," *Phytotherapy Research*, vol. 31, no. 3, pp. 507–515, 2017.
- [45] Z.-X. Hu, L. Tong, and Y.-M. Geng, "A review on pharmacological activities and preparations of luteolin," *Clinical Journal of Chinese Medicine*, vol. 14, no. 10, pp. 141–145, 2022.
- [46] Q. Yu and G.-Z. Wu, "Research progress of anti-inflammatory properties of luteolin," *Journal of Pharmaceutical Research*, vol. 38, no. 02, pp. 108–111, 2019.
- [47] Z.-B. W. J.-Z. Wang, "Progress in mechanism prediction and pharmacology of naringenin in the treatment of CHD," *Information on Traditional Chinese Medicine*, vol. 38, no. 4, pp. 77–81, 2021.
- [48] M.-T. Huang, *Naringin Inhibits Platelet Activation and Arterial Thrombosis through P2Y12 Receptor Signaling Pathway*, Guanzhou University of Traditional Chinese Medicine, Guanzhou, China, 2017.
- [49] S. B. Wang, J. Y. Jang, Y. H. Chae et al., "Kaempferol suppresses collagen-induced platelet activation by inhibiting NADPH oxidase and protecting SHP-2 from oxidative inactivation," *Free Radical Biology and Medicine*, vol. 83, pp. 41–53, 2015.
- [50] P. Yan, C. Sun, J. Ma, Z. Jin, R. Guo, and B. Yang, "MicroRNA-128 confers protection against cardiac microvascular endothelial cell injury in coronary heart disease via negative regulation of IRS1," *Journal of Cellular Physiology*, vol. 234, no. 8, pp. 13452–13463, 2019.
- [51] Z. Li, X. Wu, L. Gu et al., "Long non-coding RNA ATB promotes malignancy of esophageal squamous cell carcinoma by regulating miR-200b/Kindlin-2 axis," *Cell Death & Disease*, vol. 8, no. 6, p. e2888, 2017.
- [52] X. Yu, Y. Qi, T. Zhao et al., "NGF increases FGF2 expression and promotes endothelial cell migration and tube formation through PI3K/Akt and ERK/MAPK pathways in human chondrocytes," *Osteoarthritis and Cartilage*, vol. 27, no. 3, pp. 526–534, 2019.
- [53] D.-Y. Wu, Y. Deng, and J. Hao, "PI3K/AKT/mTOR signaling mediates baicalin-inhibited proliferation in hypertrophic scar fibroblast," *Chinese Journal of Biochemistry and Molecular Biology*, vol. 30, no. 01, pp. 60–67, 2014.
- [54] T. Li, D.-J. Wang, and Y.-Y. Xu, "Metformin regulates macrophage differentiation and inhibits formation of atherosclerosis by activating AMPK/STAT3 pathway in mice," *Chinese Journal of Arteriosclerosis*, vol. 30, no. 04, pp. 287–294, 2022.
- [55] J. Mercer, N. Figg, V. Stoneman, D. Braganza, and M. R. Bennett, "Endogenous p53 protects vascular smooth muscle cells from apoptosis and reduces atherosclerosis in ApoE knockout mice," *Circulation Research*, vol. 96, no. 6, pp. 667–674, 2005.
- [56] F. Zuo, C. Pam, and Y.-P. Li, "Latest research progress of NRG1-ERBB pathway in treatment of coronary heart disease," *Journal of Practical Traditional Chinese Internal Medicine*, vol. 35, no. 09, pp. 76–79, 2021.
- [57] A. Sanches-Silva, L. Testai, S. F. Nabavi et al., "Therapeutic potential of polyphenols in cardiovascular diseases: regulation of mTOR signaling pathway," *Pharmacological Research*, vol. 152, Article ID 104626, 2020.
- [58] Y. Li, J. Feng, S. Song et al., "gp130 controls cardiomyocyte proliferation and heart regeneration," *Circulation*, vol. 142, no. 10, pp. 967–982, 2020.
- [59] H. Hagar and M. W. Al, "Betaine supplementation protects against renal injury induced by cadmium intoxication in rats: role of oxidative stress and caspase-3," *Environmental Toxicology and Pharmacology*, vol. 37, no. 2, pp. 803–811, 2014.
- [60] Y. Zhang, X. Yang, F. Bian et al., "TNF-alpha promotes early atherosclerosis by increasing transcytosis of LDL across endothelial cells: crosstalk between NF-kB and PPAR-gamma," *Journal of Molecular and Cellular Cardiology*, vol. 72, pp. 85–94, 2014.
- [61] S. L. Pompura and M. Dominguez-Villar, "The PI3K/AKT signaling pathway in regulatory T-cell development, stability, and function," *Journal of Leukocyte Biology*, vol. 103, no. 6, pp. 817–823, 2018.
- [62] R. Rong and X.-J. Xiao, "Erythropoietin pretreatment suppresses inflammation by activating the PI3K/Akt signaling pathway in myocardial ischemia-reperfusion injury," *Experimental and Therapeutic Medicine*, vol. 10, no. 2, pp. 413–418, 2015.
- [63] J. Liu, P. Xu, D. Liu et al., "TCM regulates PI3K/Akt signal pathway to intervene atherosclerotic cardiovascular disease," *Evidence-based Complementary and Alternative Medicine*, vol. 2021, Article ID 4854755, 11 pages, 2021.
- [64] Y. Meng, H. Qin, and Q. Ma, "Study on the mechanism of Qishen capsule improving ApoE-/- atherosclerosis mice via PI3K/AKT signaling pathway," *Clinical Journal of Medical Officer*, vol. 48, no. 08, pp. 932–934, 2020.
- [65] A. Carrizzo, G. M. Conte, E. Sommella et al., "Novel potent decameric peptide of spirulina platensis reduces blood pressure levels through a PI3K/AKT/eNOS-Dependent mechanism," *Hypertension*, vol. 73, no. 2, pp. 449–457, 2019.
- [66] X.-Y. Li, *Correlation between Serum Ox-HDL and IL-1β in Patients with Coronary Heart Disease*, Shanxi Medical University, Shanxi, China, 2018.
- [67] B. D. Manning and A. Toker, "AKT/PKB signaling: navigating the network," *Cell*, vol. 169, no. 3, pp. 381–405, 2017.